Open access • Journal Article • DOI:10.1103/PHYSREVA.48.132

Continuous position measurements and the quantum Zeno effect. — Source link

M. J. Gagen, Howard M. Wiseman, Gerard J. Milburn

Published on: 01 Jul 1993 - Physical Review A (American Physical Society)

Topics: Quantum Zeno effect, Master equation, Quantum system, Schrödinger equation and Position (vector)

Continuous position measurements and the quantum Zeno effect

M.J. Gagen,* H.M. Wiseman,† and G.J. Milburn‡
Department of Physics, University of Queensland, Queensland 4072, Australia
(Received 15 January 1993)

We present a model of continuous (in time) position measurements on a quantum system using a single pseudoclassical meter. The nonselective evolution of the system is described by a master equation which is identical to that obtained from previous models. The selective evolution is described by a stochastic nonlinear Schrödinger equation. The significance of this equation is that the stochastic term has a physical interpretation. By carefully choosing the parameters which define the meter and the system-meter coupling, we obtain a meter pointer with well-defined position which undergoes fluctuations. This "jitter" in the pointer position gives rise to the stochastic dynamical collapse of the system wave function. By the inclusion of feedback on the meter, the pointer is made to relax towards an appropriate readout. We apply this model to the selective measurement of the position of a particle in a double-well potential. In contrast to a recent claim [H. Fearn and W. E. Lamb, Jr., Phys. Rev. A **46**, 1199 (1992)] we show that truly continuous position measurements lead to a quantum Zeno effect in certain parameter regimes. This is manifested by the changing of the particle dynamics from coherent tunneling between the well minima to incoherent flipping, as in a random telegraph. As the measurement strength increases, the average length of time the particle remains stuck in one well increases proportionally.

PACS number(s): 03.65.Bz,02.50.-r

I. INTRODUCTION

The simplest model for position measurement is of course the projection postulate [1]. This is defined as follows (in one dimension for simplicity). A measurement of position X of a particle at time t has the result $X = x$ with probability $|\psi(x)|^2$, where $\psi(X)$ is the wave function of the particle in the position representation. Immediately after the measurement, the particle is in a position eigenstate with wave function $\sqrt{\delta(X-x)}$. This model of measurement is unrealistic for a number of reasons, the most important of which is that the projected system state has infinite energy. Also, it would be desirable to have a model which would allow measurements continuous in time, as this allows the investigation of the so-called quantum Zeno effect [2–4]. This is the purely quantum phenomenon by which continuous measurement may arrest the evolution of the system.

A fruitful approach to develop more realistic measurement models is to expand the Hilbert space used to include a meter which is coupled to the particle. The meter is thus treated formally as a quantum-mechanical system, but is expected to have some properties which makes it behave in a pseudoclassical manner. Of course, this does not solve the quantum measurement problem. It is still necessary to use the projection postulate on the meter. However, by moving this cut one step away from the system, we can hope for a more refined model. In the construction of our model, we were guided by three conditions which we believe apply to real laboratory meters: (a) the system interacts with a single meter over time, (b) the meter pointer is described by a continuous readout parameter, and (c) the system evolution is well defined for any trajectory of the meter pointer.

The measurement model which we construct in Sec. II shares much in common with an earlier model of Caves and Milburn [5]. The most significant difference is that we have a single, well-defined pointer variable [as defined in conditions (a) and (b) above], rather than a succession of meters which are thrown away after each measurement. In the meter Hamiltonian we include a term, linear in the meter momentum, which shifts the pointer position. When the amount of the shift is made to depend on the results of measurement, this becomes a feedback stabilization of the pointer. The net effect is to cause the pointer to relax to a stable position determined by the measured system variable. Also, we derive an explicit stochastic Schrödinger equation for the wave function of the system conditioned on the meter readout. Similar differential equations have been proposed previously in the context of measurement theory [6–10]. However, these have not been derived from a physical model for measurement involving a meter pointer, and hence the system wave function obeying these stochastic Schrödinger equations does not have a clear interpretation as a state conditioned on the meter readout.

In Sec. III, we apply the position measurement model to a simple and interesting case: a particle in a quartic double-well potential. Of particular interest is how the measurement process disturbs the tunneling of the low-energy particle from one well to the other. We show that, in some experimental regimes, the quantum Zeno effect can be observed. This is manifest in the behavior of the particle, which ceases to tunnel coherently between the

wells, and instead flips incoherently between them in the manner of a random telegraph. The length of time the particle remains stuck in one well is proportional to the measurement strength. This result is in contrast to a recent claim by Fearn and Lamb [11] to the effect that there was no appearance of the quantum Zeno effect in the tunneling behavior of a particle in a double-well system. As well as the full ponderomotive model, we consider the two-state approximation which is valid for particles with energy much lower than the barrier potential. The two states correspond to the particle localized in the left or right well. This approximation is useful because the nonselective evolution is completely solvable, and the relation to the quantum Zeno effect has been studied in depth [12]. In addition, we take the opportunity to compare our measurement model with the two-level example considered recently by Bonilla and Guinea [13].

The act of measuring the position of the particle causes its energy on average to increase linearly with time. The particle energy will eventually become greater than the potential barrier, and then the two-level approximation will cease to give insight into the behavior of the system. The more accurate the measurement, the shorter the time over which the approximation will be valid. For weak measurements, this time may be much longer than the tunneling time. For very strong measurements, there is no Zeno effect. Such measurements still cause the position variance of the wave packet to be small, but the energetic wave packet moves violently rather than being pinned to its starting point.

II. MODEL FOR CONTINUOUS SELECTIVE POSITION MEASUREMENTS

Consider a pseudoclassical meter with position and momentum operators $\hat{Q}$ and $\hat{P}$, respectively. We use the description pseudoclassical as we take the mass of the meter to infinity and the commutator $[\hat{Q},\dot{\hat{Q}}] \to 0$. Thus the position of the meter $X(t) = \langle\hat{Q}\rangle(t)$ is always well defined, as is its velocity. We describe the state of the meter by the ket $|X(t),P(t)\rangle$, which has the following form in the Q representation ($\hat{Q}|Q\rangle = Q|Q\rangle$):

$$\langle Q|X(t),P(t)\rangle = (2\pi\sigma^2)^{-\frac{1}{4}}\exp\left\{-\frac{[Q-X(t)]^2}{4\sigma^2} + \frac{i}{\hbar}QP(t)\right\}. \quad (2.1)$$

Here, the spread in the position σ will later be assumed to be arbitrarily small so that the meter wave function is well represented by its mean position $X(t)$ and mean momentum $P(t)$. For most of this paper, we will need only the states $|X(t)\rangle \equiv |X(t),0\rangle$. In this state, the meter has an average momentum of zero. The meter moves only due to its interaction with the system, the Hamiltonian of which commutes with $\hat{P}$. This assumption is not essential, but does make the analysis simpler. The completeness relation for the states of the meter is

$$I = \int \frac{dX\,dP}{2\pi\hbar}|X,P\rangle\langle X,P|, \quad (2.2)$$

where I is the identity operator. We will later require the inner product between two states of zero momentum. This can readily be shown to be

$$C(X,Y) = \langle X|Y\rangle = \exp\left[-\frac{(X-Y)^2}{8\sigma^2}\right]. \quad (2.3)$$

We now turn our attention to the system, a particle with position operator $\hat{x}$. The system Hamiltonian H_0 is left arbitrary for the time being. The interaction between the system and the meter is of the form

$$\hat{H}_{SM} = \gamma\hat{P}[\hat{x}-F], \quad (2.4)$$

where F is an arbitrary real number. In the case where $F = 0$ then this system-meter interaction is that considered by von Neumann [14] and later by Refs. [4,5,12]. This interaction translates the position of the meter by an amount proportional to the average position of the system. In the case where $F \neq 0$ then this term in the interaction causes a displacement of the meter coordinate. It has no effect on the dynamics of the system.

The state of the system and meter at time t is taken to be

$$|\Phi(t)\rangle = |X(t)\rangle \times |\Psi(t)\rangle, \quad (2.5)$$

where $|\Psi(t)\rangle$ is a system ket. Then under the coupling of Eq. (2.4), and the free-system Hamiltonian H_0, the combined state at time $t+\tau$ (for τ infinitesimal) is

$$|\Phi(t+\tau)\rangle = \exp\left\{-\frac{i\gamma\tau}{\hbar}\hat{P}\,[\hat{x}-F]\right\}|X(t)\rangle \times|\Psi_0(t+\tau)\rangle_S, \quad (2.6)$$

where the state of the system at time $t+\tau$ is approximately

$$|\Psi_0(t+\tau)\rangle = \left(1-\frac{i\tau}{\hbar}H_0\right)|\Psi(t)\rangle. \quad (2.7)$$

This evolution of the combined system and meter is purely unitary. The meter has undergone the desired translation due to the interaction with the system. The system has undergone its usual free evolution and has a measurement backaction operating on it due to the interaction with the meter.

Now since the meter is pseudoclassical it should always be describable by $X(t)$ with uncertainty σ. Its large mass ensures that it will be negligibly perturbed by a classical measurement process. Thus the effect of observing the meter state should be well modeled by a projection onto a new Gaussian state $|X(t+\tau),P(t+\tau)\rangle$. This step (using the projection postulate) is necessary at some stage in the measurement chain in order to describe the result of the measurement. The positioning of this formal procedure (the Heisenberg cut [15]) is essentially arbitrary, but the higher up the chain from the system to the observer the cut is placed the more accurate the model of the measurement will be. Placing the cut after the meter will yield a good description of the behavior of the system and the meter.

The reasons we choose to project the meter onto a

Gaussian state rather than an eigenstate of position as in previous models [5] are twofold. Firstly, it is more realistic—creating a position eigenstate requires an infinite amount of energy. Secondly, we wish to use the meter again and so have it prepared in a Gaussian state as in the previous measurement period. Following the projection of the meter at time $t+\tau$, the meter will have, in general, a nonzero mean momentum equal to the observed value $P(t+\tau)$. This is an undesirable effect and can be eliminated by the action of a unitary displacement operator $D[-P(t+\tau)] = \exp[-iP(t+\tau)\hat{Q}]$. Physically, this models the damping of the meter momentum, so that

$$D[-P(t+\tau)]|X(t+\tau), P(t+\tau)\rangle = |X(t+\tau)\rangle.$$

It does not affect the system, nor the system-meter entanglement which involves only $X(t+\tau)$. Thus, the state of the system and meter, given the readout result $X(t+\tau)$, is

$$\begin{aligned}|\Phi_c(t+\tau)\rangle &= [P(X)]^{-1/2}|X(t+\tau)\rangle\langle X(t+\tau)| \\ &\quad\times \exp\left\{-\frac{i\gamma\tau}{\hbar}\hat{P}\,[\hat{x}-F]\right\} \\ &\quad\times|X(t)\rangle|\Psi_0(t+\tau)\rangle \\ &= [P(X)]^{-1/2}|X(t+\tau)\rangle \otimes |\tilde{\Psi}_c(t+\tau)\rangle, \quad (2.8)\end{aligned}$$

where we have defined an unnormalized system ket

$$\begin{aligned}|\tilde{\Psi}_c(t+\tau)\rangle &= C(X(t+\tau), X(t)+\gamma\tau[\hat{x}-F]) \\ &\quad\times|\Psi_0(t+\tau)\rangle, \quad (2.9)\end{aligned}$$

where $C(X,Y)$ is as defined in Eq. (2.3). Here we use the subscript c to indicate that the state of the system is conditioned on the entire history of the readout variable $X(t)$. That is, we are considering selective evolution of the system, hence the possibility of using a wave function rather than density-operator description. The normalization term $P(X)$ is equal to the probability of obtaining the result $X(t+\tau)$. It is given by

$$P(X) = \langle\tilde{\Psi}_c(t+\tau)|\tilde{\Psi}_c(t+\tau)\rangle. \quad (2.10)$$

The mean and variance for the distribution of $X(t+\tau)$ are

$$\langle X(t+\tau)\rangle = X(t) + \gamma\tau[\langle\hat{x}\rangle_c - F], \quad (2.11)$$

$$V(X(t+\tau)) = 2\sigma^2 + \gamma^2\tau^2 V(\hat{x}). \quad (2.12)$$

In order to obtain smooth evolution of the *system*, we will show shortly that the following measurement parameter must be finite in the limit $\tau \to 0$:

$$\Gamma = \frac{\gamma^2\tau}{8\sigma^2}. \quad (2.13)$$

The implication of this for the *meter* evolution is that in Eq. (2.12) the $2\sigma^2$ term will dominate in the limit $\tau \to 0$. In this case $X(t+\tau)$ is well approximated by a Gaussian random variable, and can be replaced by

$$X(t+\tau) = X(t) + \gamma\tau\left(\langle\hat{x}\rangle_c(t) - F + \frac{1}{2\sqrt{\Gamma}}\xi(t)\right), \quad (2.14)$$

where $\xi(t)$ indicates Gaussian noise of standard deviation $1/\sqrt{\tau}$. Since this term is independent from one τ increment to the next, in the limit $\tau \to 0$ it can be modeled by white noise $\xi(t)$ with $\langle\xi(t)\xi(t')\rangle = \delta(t-t')$. Note that F, which we have so far left arbitrary, can be chosen to be a function of $X(t)$, the previous measurement result. This allows feedback on the meter position to prevent the meter pointer from becoming unbounded, which was an undesirable feature of previous models [5].

It is evident that Eq. (2.14) describes a driven meter with position diffusion, providing that γ is finite as $\tau \to 0$. This is a natural choice as we wish to follow the dynamics of the meter pointer. However, it is not a necessary assumption. The choice of scaling of γ fixes the scaling of σ if Γ is to remain finite. The various possibilities can be labeled by a real number n, as shown in Table I.

Our choice corresponds to $n = 1/2$, in which the position uncertainty of the meter goes to zero with τ. This is consistent with our earlier statement that the position of the meter is defined arbitrarily accurately.

Taking the limit $\tau \to 0$ in Eq. (2.14), we see that the meter position $X(t)$ obeys the following stochastic differential equation:

$$\dot{X}(t) = \gamma\left[\langle\hat{x}\rangle_c(t) - F + \frac{1}{2\sqrt{\Gamma}}\xi(t)\right]. \quad (2.15)$$

Here the effect of the feedback term F is evident. In this paper we take $F = X(t)$ and this corresponds to the meter pointer relaxing at rate γ to the conditioned system mean $\langle\hat{x}\rangle_c(t)$. This is the motivation for the original Hamiltonian coupling between the meter and the system: it allows the position of the system to be read (however inaccurately) from the position of the meter pointer. Previous models [5] have treated the case where $F = 0$, whereby the information about the system operator of interest is encoded in the *velocity* of the meter pointer, and an experimenter would have to extract this information explicitly. The choice of the function F has no effect on the system dynamics.

In addition to relaxing towards its appropriate value, the meter pointer undergoes a "jitter" due to the noise term $\xi(t)$ in Eq. (2.15). The size of this jitter can be made small by taking the limit $\gamma \ll \Gamma$. However, as we will show [Eq. (2.20)], this would mean that the system would collapse towards a position eigenstate on a time scale Γ^{-1} much faster than the time scale γ^{-1} on which the meter could respond. There is thus an obvious trade off between the jitter and the response of the meter.

TABLE I. A finite parameter $\Gamma = \gamma^2\tau/8\sigma^2$ in the limit $\tau \to 0$ gives smooth system evolution. Whether this also gives smooth evolution of the meter pointer $X(t)$ depends on how γ and σ are scaled. The scaling can be defined by a real parameter n. Two scalings of interest are given, the first being that used in this paper and the second corresponding to the model of Caves and Milburn [5]

n	$\sigma \sim \tau^n$	$\gamma \sim \tau^{n-1/2}$	$\dot{X}(t) \sim \tau^{n-1/2}$
$\frac{1}{2}$	$\sqrt{\tau}$	1	well defined
$-\frac{1}{2}$	$1/\sqrt{\tau}$	$1/\tau$	not defined

We return now to the evolution of the system, conditioned on the meter readout $X(t)$. From Eq. (2.8), the combined state of the system and meter at time $t+\tau$ is a decoupled one, as it was at time t. We can thus write the new conditioned system state at time $t+\tau$ as

$$|\Psi_c(t+\tau)\rangle = [P(X)]^{-1/2}|\tilde{\Psi}_c(t+\tau)\rangle, \tag{2.16}$$

where the unnormalized ket $|\tilde{\Psi}_c(t+\tau)\rangle$ is defined in Eq. (2.9).

This result can be simplified by substituting for the meter evolution [Eq. (2.14)] and using Eq. (2.3) to evaluate the inner product in Eq. (2.10). This gives

$$|\Psi_c(t+\tau)\rangle = [P(X)]^{-1/2} e^{-\Gamma\tau[\hat{x}-\langle\hat{x}\rangle_c-\frac{1}{2\sqrt{\Gamma}}\xi(t)]^2} \times|\Psi_0(t+\tau)\rangle. \tag{2.17}$$

As we have obtained an exponential that is first order in τ we can obtain a stochastic differential equation for the evolution of the system. When we expand the exponential (carefully because of the noise term) we obtain

$$\frac{d}{dt}|\Psi_c(t)\rangle = \left(-\frac{i}{\hbar}H_0 - \frac{\Gamma}{2}[\hat{x}-\langle\hat{x}\rangle_c]^2 + \sqrt{\Gamma}\xi(t)[\hat{x}-\langle\hat{x}\rangle_c]\right)|\Psi_c(t)\rangle. \tag{2.18}$$

It is interesting to note that this stochastic Schrödinger equation is identical to that resulting from homodyne detection [16] with the replacement $\hat{a} \to \hat{x}$. Similar equations have also been considered in Refs. [6–10,17,18]. The significance of the approach considered here is that we have an unravelling of the master equation as an ensemble of stochastic, continuous trajectories for the state vector of the system. Each of these trajectories has an explicit interpretation in terms of the readout of a continuous pseudoclassical meter. This we believe to be a feature that may have important applications.

Later in this paper, we will be comparing our model with that proposed by Bonilla and Guinea [13]. The advantage of our model is that the collapse of the system wave function is a natural outcome of the measurement process, as might be expected. This is in contrast to their approach where a system-environment interaction is introduced in order to achieve a collapse to an eigenstate of the measured quantity. Also, their model does not guarantee correct measurement statistics. That our model does guarantee this is evident from the nonselective master equation (2.20) which we derive below. If the free evolution from H_0 can be ignored, then the statistics of the measured quantity $\hat{x}$ remains unchanged. Since an eigenestate of $\hat{x}$ is also an eigenstate of the stochastic evolution generator [Eq. (2.18)], again ignoring H_0, this shows that the system will end up in an eigenstate with the appropriate probability. It is when H_0 cannot be ignored that the superiority of our model over the projection postulate emerges.

The stochastic Schrödinger equation (2.18) is easily shown to be equivalent to the following stochastic master equation for the selective evolution of the conditioned density operator:

$$\dot{\rho}_c(t) = \frac{-i}{\hbar}[H_0,\rho_c] - \frac{\Gamma}{2}[\hat{x},[\hat{x},\rho_c]] + \sqrt{\Gamma}\xi(t)(\hat{x}\rho_c + \rho_c\hat{x} - 2\langle\hat{x}\rangle_c\rho_c). \tag{2.19}$$

This stochastic master equation is conditioned on the entire history of the meter readout $X(t)$. If we were only interested in the nonselective evolution of the system, then we would have to discard all knowledge of the evolution of the system. This is achieved in the usual manner of averaging over all possible meter readouts at all times t. In our case this simply amounts to averaging over the stochastic term in Eq. (2.19), which gives zero since $\xi(t)$ is independent of the system state at time t. The nonselective master equation for the system is thus

$$\dot{\rho}_{\rm NS}(t) = \frac{-i}{\hbar}[H_0,\rho_{\rm NS}] - \frac{\Gamma}{2}[\hat{x},[\hat{x},\rho_{\rm NS}]]. \tag{2.20}$$

This is the expected double-commutator form of the nonselective master equation which usually arises from system-meter couplings which do not disturb the measured quantity such as that employed in Eq. (2.4).

If H_0 can be written as

$$H_0 = \frac{\hat{p}^2}{2m} + V(\hat{x}), \tag{2.21}$$

then the nonselective master equation (2.20) yields

$$\frac{d}{dt}\langle\hat{x}\rangle = \frac{1}{m}\langle\hat{p}\rangle, \tag{2.22}$$

$$\frac{d}{dt}\langle\hat{p}\rangle = -\langle V'(\hat{x})\rangle. \tag{2.23}$$

That is to say, the measurement term does not affect the Ehrenfest relations. If V is a polynomial up to second order in $\hat{x}$, then these equations are closed. Thus the measurement has no effect on the mean value of $\hat{x}$ if the particle moves in a linear or quadratic potential. This means, for example, that no Zeno effect could be manifest in such systems. In the following section we examine motion in a quartic potential. It can be shown that the effect of the measurement first appears with the fifth-order derivative

$$\frac{d^5}{dt^5}\langle\hat{x}\rangle \sim -24c\Gamma\langle\hat{x}\rangle, \tag{2.24}$$

where c is the coefficient of $\hat{x}^4$ in $V(\hat{x})$.

III. TUNNELING IN A DOUBLE-WELL POTENTIAL

In this section we apply our model to the measurement of the position of a particle in a double-well potential. We demonstrate the measurement regimes in which the quantum Zeno effect will be apparent.

The Hamiltonian for a particle in a quartic double-well potential is

$$H_0 = \frac{\hat{p}^2}{2m} - \frac{m\omega_0^2}{4}\hat{x}^2 + \frac{m^2\omega_0^4}{64D}\hat{x}^4, \tag{3.1}$$

where m is the mass of the particle, D is the height of the potential barrier between the minima, and ω_0 is the frequency of oscillation of the particle in one of the minima (approximated as a quadratic potential). Such a double-well system has been extensively studied (see Refs. [19,20] and references therein). We transform to natural units by setting $m = \hbar = \omega_0 = 1$. We obtain for the Hamiltonian

$$H_0 = \tfrac{1}{2}\hat{p}^2 - \tfrac{1}{4}\hat{x}^2 + \beta\hat{x}^4, \tag{3.2}$$

where $\beta = 1/(64D)$ and D is now dimensionless.

The double-well potential has alternating odd and even eigenstates. Those with energies well below the barrier potential will be nearly degenerate in pairs, and superposition of these pairs can be constructed so as to give states well localized in the left or the right well. Such states will be like coherent states of a harmonic oscillator centered on the minima of the respective wells. In this paper we set the depth $D = 1$, which has the eigenvalue structure for the double well shown in Table II.

We consider the first two such localized states, $|+\rangle$, and $|-\rangle$, found in the right- and left-hand wells, respectively. These states are given by

$$|\pm\rangle = \frac{1}{\sqrt{2}}\left(|1\rangle \pm |2\rangle\right). \tag{3.3}$$

We choose as our initial state $|-\rangle$ and monitor the time the particle takes to tunnel to the right-hand well when its state is $|+\rangle$. This tunneling occurs under free evolution, and the time taken T_t is given by the inverse energy difference between the states $|1\rangle$ and $|2\rangle$

$$T_t = \frac{\pi}{\Delta}. \tag{3.4}$$

We see this tunneling behavior clearly in Fig. 1(a). Here we show the evolution of the probability density for the system position $\hat{x}$ under free evolution. With purely unitary evolution, the system is completely equivalent to a two-level system, because of the chosen initial conditions. In Fig. 1(b) we show the time evolution of the average position of the particle and the position standard deviation. The numerical technique we used to simulate the behavior of the particle in the double-well potential is described in the Appendix.

TABLE II. The eigenvalue structure of the double well treated in this paper with depth $D = 1$. Also shown is the energy difference between the bottom pair of states Δ and the associated tunneling time T_t.

$\|i\rangle$	E_i	Δ	T_t
$\|1\rangle$	-0.54980	0.023923	131.32
$\|2\rangle$	-0.52587		
$\|3\rangle$	0.09262		
$\|4\rangle$	0.39333		

A. Numerical solution of exact system

It is obvious that vanishingly weak measurements ($\Gamma \to 0$) will not manifest the quantum Zeno effect. In this limit there is no measurement backaction on the system. However, it is also the case for the system considered here that too strong a measurement process also makes the quantum Zeno effect unobservable. This arises as the measurement backaction on the system tends to increase the particles energy. A highly energetic particle will not tunnel through the middle barrier; rather, it will pass over it. If we wish to observe the quantum Zeno effect, we must limit the measurement backaction on the system.

The measurement regime to demonstrate the Zeno effect can be established by considering a nonselective measurement process. At any time the average energy of the particle is given by Eqs. (2.20) and (3.2) as

$$\dot{E}_{\rm NS} = \mathrm{tr}(H_0\dot{\rho}_{\rm NS}) = \frac{\Gamma}{2}. \tag{3.5}$$

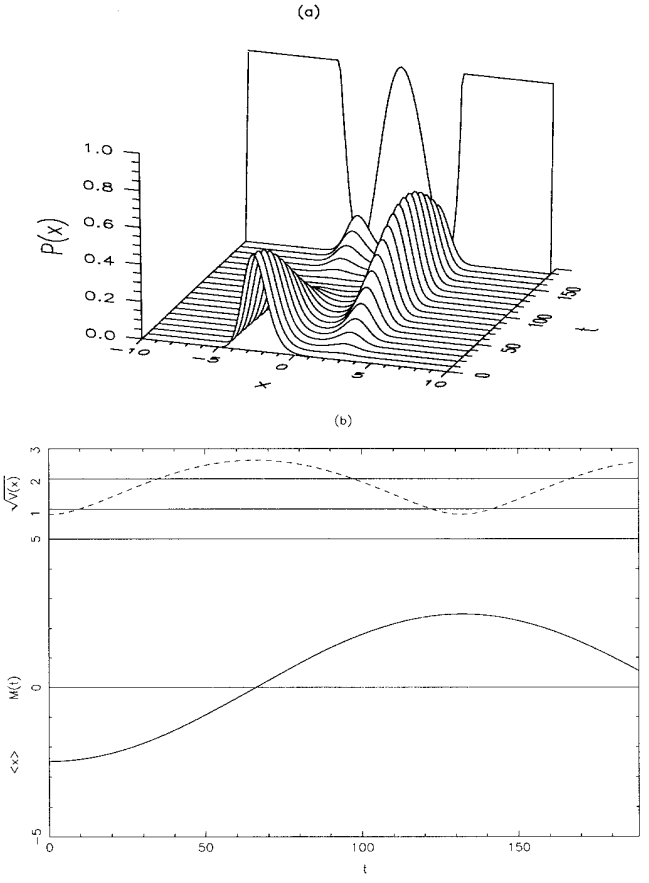

FIG. 1. Free evolution with $\Gamma = 0$. (a) Plot of the time evolution of probability density for the system position $\hat{x}$ of a particle undergoing free evolution in a double-well potential (shown at the rear of the plot). With $\Gamma = 0$, the particle coherently tunnels from the left to the right well. (b) Plot the time evolution of the average position of the particle $\langle\hat{x}\rangle_c$ (heavy line) and the position standard deviation $V(x)$ (dashed line) for the same value of Γ as in (a).

With the initial condition $E_{\rm NS}(0) = E_- = (E_1 + E_2)/2$ we then have

$$E_{\rm NS}(t) = E_- + \frac{\Gamma}{2}t. \tag{3.6}$$

In this paper we wish to observe tunneling behavior on a time scale of about one tunneling time T_t. For the double-well system we are using (see Table II) tunneling will occur as long as we do not excite level $|3\rangle$. We require that $E_{\rm NS}(T_t) \ll E_3$. This constraint gives

$$\Gamma \ll \frac{2}{T_t}(E_3 - E_-) \sim \Delta. \tag{3.7}$$

We see that the measurement strength must scale inversely with the time over which we wish to see tunneling behavior. Of course, any measurement interaction with $\Gamma > 0$ will eventually excite the particle enough to leave the tunneling regime. Once the particle is sufficiently energetic, the quantum Zeno effect will not be observable.

From the two-level approximation in the next section, it can be shown that the Zeno effect will exist only for

$$\Gamma \gtrsim \frac{\Delta}{8D}. \tag{3.8}$$

The two-level approximation is strictly only valid for $D \gg 1$. There is thus a parameter region where the Zeno effect may appear : $\Delta/8D \lesssim \Gamma \ll \Delta$. For the well considered in this paper ($D = 1$), we require $0.003 \lesssim \Gamma \ll 0.01$. This window is rather narrow but is nevertheless present as our numerical results show. As $D \to \infty$, the Zeno effect would be manifest over a large range of measurement parameter Γ. The reason that we use $D = 1$ rather than $D \gg 1$ as would be desirable is that the tunneling time increases like $\exp(16D/3)$ for large D [21], which would make numerical simulations prohibitively time consuming.

The selective evolution of the particle wave function under position measurements is given by Eq. (2.18) with H_0 given by Eq. (3.2). We gradually increase the effectiveness of our measurement, and plot typical trajectories. In each of these figures we show (a) a plot of the probability density for the position of the particle, and (b) the average position of the particle (heavy line), the readout meter variable (dotted line), and the standard deviation in the position of the particle (dashed line). The readout meter parameters have been set fixed with $\gamma = 0.05$ and $F = X(t)$. (See the Appendix for details of the numerical method used.)

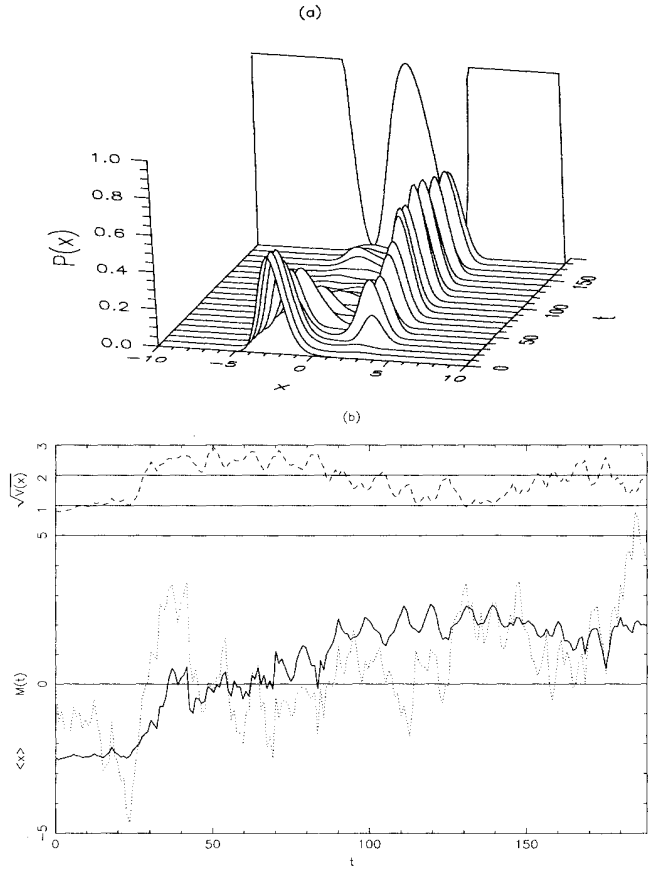

FIG. 2. Random-walk regime with $\Gamma = 0.001$. (a) As in Fig. 1(a), with $\Gamma = 0.001$. The coherent tunneling has a "random walk" added. (b) As in Fig. 1(b). The meter readout is shown by a dotted line. Since $\gamma = 0.05$, the "jitter" in the meter is large.

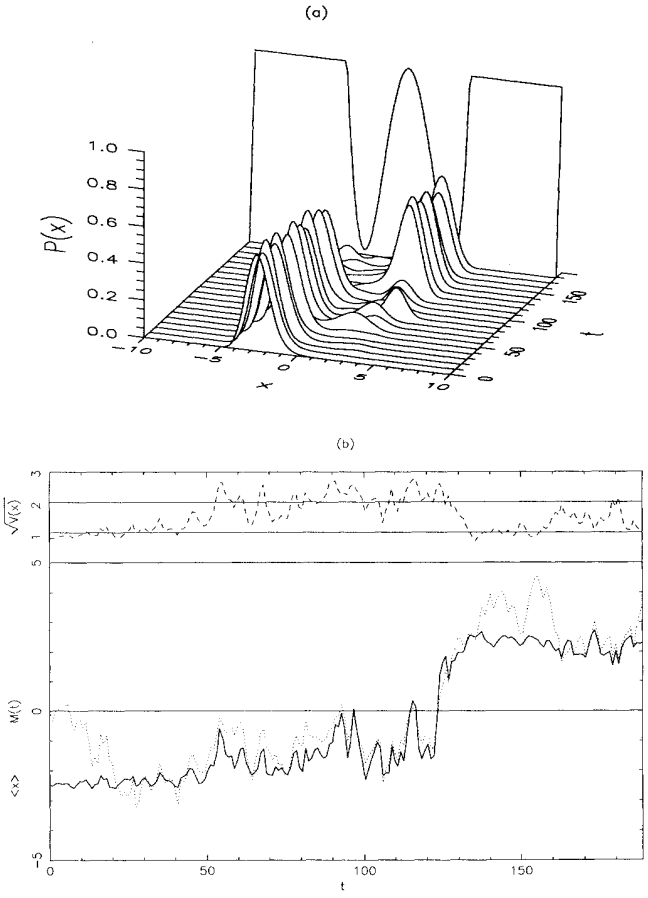

FIG. 3. Random-telegraph regime with $\Gamma = 0.003$. (a) As above with $\Gamma = 0.003$. The particle undergoes a random-telegraph-type evolution from one minima to the other. (b) As above.

In Fig. 2, $\Gamma = 0.001$ and the particle undergoes a diffusive random walk. This is seen most clearly in the average-position evolution. The"walk" is dominated by the free unitary evolution. We note the large scale of the "jitter" in the meter readout in Fig. 2(b). With the chosen meter parameters the meter response [determined by $\gamma/\sqrt{\Gamma}$ in Eq. (2.15)] is too large. The response improves in later figures as Γ increases.

The transition to the random-telegraph regime is seen very clearly in Fig. 3 where $\Gamma = 0.003$. The particle is trapped for some considerable time in the left well, and then makes a random, and sudden transition to the right-hand well.

In Fig. 4 we are well into the regime where we manifest the quantum Zeno effect with $\Gamma = 0.005$. The behavior is fully described by a random telegraph. Further, the survival probability of the particle in the initial state is significantly enhanced. During the time of observation, the particle did not jump to the right well. This is the quantum Zeno effect. Finally we discern some squeezing in the particle's position probability density under this level of selective measurement. The squeezed particle is more energetic, and we anticipate that our two-level approximation will break down and the quantum Zeno effect ceases for stronger measurements.

In addition to the typical selective trajectory, we include in Fig. 4(c) the ensemble average evolution of the meter position and the (quantum) mean particle position. These nonselective averages were calculated using an ensemble of 40 selective runs. The results clearly show that the free evolution of the particle has been arrested in the manner of a Zeno effect. We also include a theoretical curve for the nonselective particle position. This was calculated using the two-level theory of the next section, but with the replacement of $\sqrt{8D}$ by 2.48, as the latter is a better approximation to the position of the particle when it is localized in one of the wells. It is clear that the theoretical curve is in good agreement with the numerical results (within the standard error due to the finite size of the ensemble), at least for times less than the free tunneling time $T_t \simeq 131$. This is not unexpected, as we know that the two-level approximation breaks down for times greater than T_t.

The complete breakdown of the two-level approximation is confirmed in Fig. 5, where $\Gamma = 0.01$. The particle is very energetic and is no longer trapped at the bottom of either of the minima. The backaction of the strong selective measurements is such that the particle has left the two-level regime and is energetically oscillating across the entire width of the double-well potential. In a single tunneling time T_t the particle can be found any number of times on the left- or the right-hand side of the double-well potential. The quantum Zeno effect can no longer be observed.

The behavior seen in this last plot is similar to that observed in the results of Fearn and Lamb [11]. We believe that herein lies part of the explanation as to why they failed to observe the quantum Zeno effect. Their measurement parameters were apparently chosen so that their particle became highly energetic very quickly, and so could not remain trapped in one well. In addition,

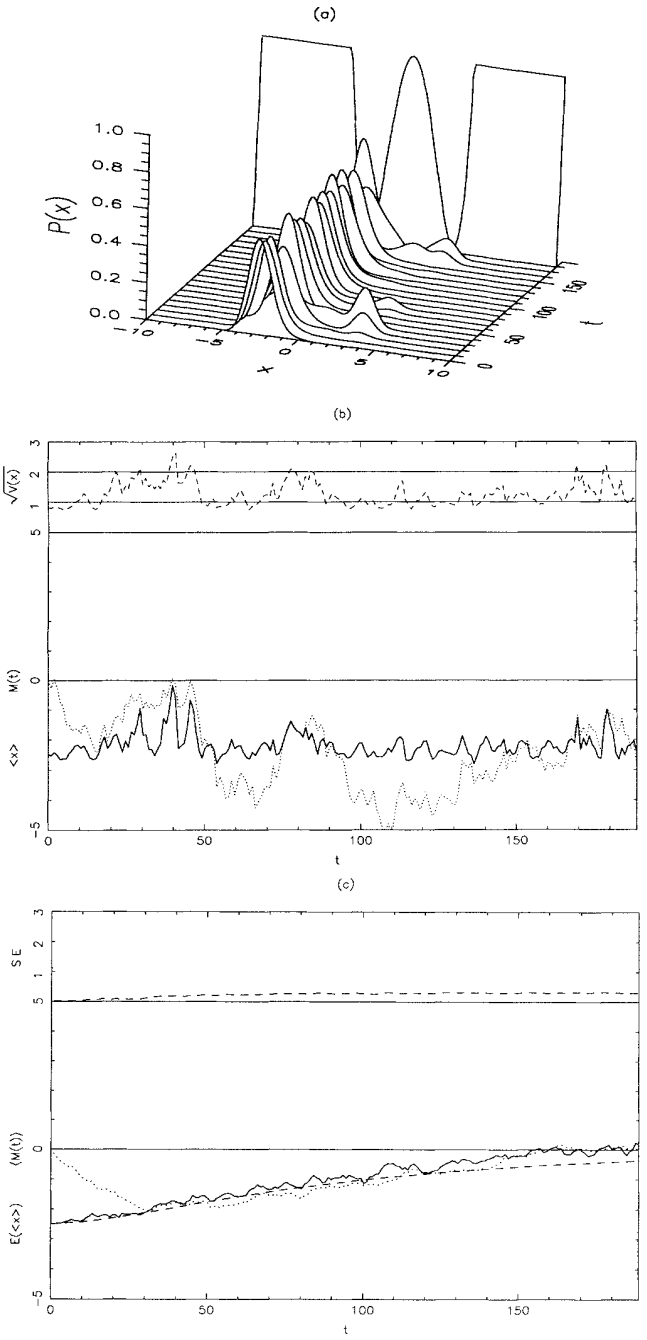

FIG. 4. The quantum Zeno effect with $\Gamma = 0.005$. (a) As above with $\Gamma = 0.005$. We see strong evidence of the quantum Zeno effect in the delayed transition from the left to the right well. The particle position is somewhat squeezed. (b) As above. (c) Plot of the ensemble average evolution of the meter position (dotted line) and the (quantum) mean particle position (solid line). These nonselective averages were calculated using an ensemble of 40 selective runs. The standard error (SE) in the mean particle position is also shown. This clearly shows that the free evolution of the particle has been arrested in the manner of a Zeno effect and is in good agreement for short times with the theoretical curve for the nonselective particle position calculated using the two-level approximation (dashed curve).

their measurement model, unlike ours, does not correspond to strictly continuous measurements, as required to see the Zeno effect. We have demonstrated that a realistic model for continuous position measurements of a particle does result in the Zeno effect in at least some experiments.

B. The two-level approximation

We have previously commented on the similarity of the free-evolution tunneling behavior of the particle to that of coherent evolution of a driven two-level system (see Refs. [19,20]). This approximation is explored in this section. Our two-level treatment has the additional advantage of allowing us to compare our measurement model directly to that considered by Bonilla and Guinea [13].

As previously indicated, we are able to use an approximate discrete two-level basis for a particle in the double-well potential provided that it has sufficiently low energy so that the occupation of the energy eigenstates is restricted to the lowest two states. This approximation effectively converts the position operator into a discrete operator with eigenvalues "left" and "right." In this pseudodiscrete system, the quantum Zeno effect can be readily manifest.

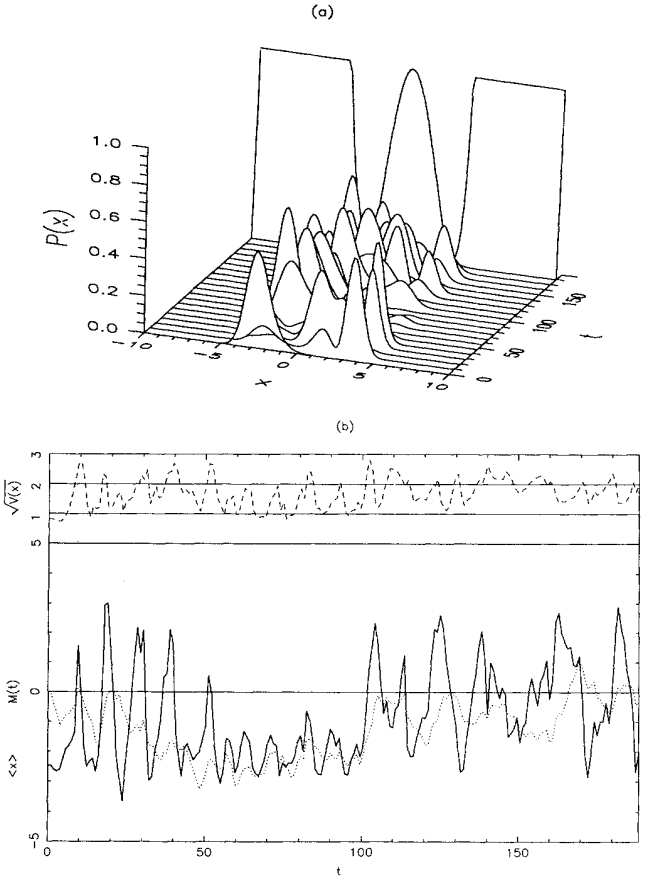

FIG. 5. The energetic-particle evolution with $\Gamma = 0.01$. (a) As above with $\Gamma = 0.01$. The particle is very energetic and is no longer trapped at the bottom of either of the minima. The measurement backaction is so strong that the particle has left the regime of the two-level approximation, so we do not expect the Zeno effect to be manifest. (b) As above. The particle is energetically oscillating across the entire width of the double-well potential. In this plot the particle can be found a number of times on the left- or the right-hand side of the double-well potential. Note that the meter is lagging behind the higher-frequency oscillations.

In the two-level approximation, we use only the states $|1\rangle, |2\rangle$ or equivalently, $|+\rangle, |-\rangle$. It can readily be shown that the free Hamiltonian of the double well is equivalent to

$$\begin{aligned} H_0 &= \frac{\Delta}{2}\begin{pmatrix} -1 & 0 \\ 0 & 1 \end{pmatrix}_{1,2} \\ &= -\frac{\Delta}{2}\begin{pmatrix} 0 & 1 \\ 1 & 0 \end{pmatrix}_{\pm} \\ &= -\Delta\hat{\sigma}_x. \end{aligned} \tag{3.9}$$

Here we use the usual Pauli matrices $\hat{\sigma}_x, \hat{\sigma}_y, \hat{\sigma}_z$ as operators in the $|\pm\rangle$ basis. The position measurement operator is

$$\begin{aligned} \hat{x} &= \sum_{i,j=1}^{\infty} \langle j|\hat{x}|i\rangle \ |i\rangle\langle j| \\ &\approx \sum_{i,j=1}^{2} \langle j|\hat{x}|i\rangle \ |i\rangle\langle j| \\ &= \langle 1|\hat{x}|2\rangle \ |2\rangle\langle 1| + \text{H.c.}, \end{aligned} \tag{3.10}$$

where H.c. means the Hermitian conjugate. In deriving the above we have made the two-level approximation and used the evenness and oddness of the eigenstates of the Hamiltonian. Given this approximation we readily show that

$$\begin{aligned} \hat{x} &\approx \sqrt{8D}\begin{pmatrix} -1 & 0 \\ 0 & 1 \end{pmatrix}_{\pm} \\ &= 2\sqrt{8D}\,\hat{\sigma}_z. \end{aligned} \tag{3.11}$$

Here $\pm\sqrt{8D}$ are the positions of the double-well minima, which for $D \gg 1$ are very close to the mean positions of the left and right wave functions.

We are interested in following the selective evolution of the particle under position measurements, and also the nonselective evolution when no account is taken of the measurement results. For convenience we rewrite the relevant evolution equations for the two-level approximation for the double-well system. The stochastic Schrödinger equation for the selective evolution of the state vector is

$$\begin{aligned} \frac{d}{dt}|\Psi_c(t)\rangle = \{&i\Delta\hat{\sigma}_x - 16D\Gamma[\hat{\sigma}_z - \langle\hat{\sigma}_z\rangle_c]^2 \\ &+4\sqrt{2D\Gamma}\xi(t)[\hat{\sigma}_z - \langle\hat{\sigma}_z\rangle_c]\}|\Psi_c(t)\rangle. \end{aligned} \tag{3.12}$$

The nonselective master equation for the two-level system is

$$\dot{\rho}_{\rm NS}(t) = i\Delta[\hat{\sigma}_x, \rho_{\rm NS}] - 16D\Gamma[\hat{\sigma}_z, [\hat{\sigma}_z, \rho_{\rm NS}]]. \tag{3.13}$$

First we consider the selective evolution of our two-level tunneling system. We define the components of the Bloch vector as

$$\begin{aligned} X(t) &= \langle \hat{\sigma}_x(t) \rangle, \\ Y(t) &= \langle \hat{\sigma}_y(t) \rangle, \\ Z(t) &= \langle \hat{\sigma}_z(t) \rangle. \end{aligned} \tag{3.14}$$

The evolution of the Bloch vector is readily shown to be

$$\frac{d}{dt}\begin{pmatrix} X \\ Y \\ Z \end{pmatrix} = \begin{pmatrix} -16D\Gamma & 0 & 0 \\ 0 & -16D\Gamma & \Delta \\ 0 & -\Delta & 0 \end{pmatrix}\begin{pmatrix} X \\ Y \\ Z \end{pmatrix} + 8\sqrt{2D\Gamma}\xi(t)\begin{pmatrix} -XZ \\ -YZ \\ \frac{1}{4} - Z^2 \end{pmatrix}. \tag{3.15}$$

This equation has no stable points for the case where $\Delta, \Gamma > 0$. However, we gain an understanding of the dynamics by considering each term separately. As for the nonselective case, the deterministic term has stable point $X = Y = Z = 0$, representing a fully mixed state. In contrast, the noise term has stable point $X = Y = 0$, $Z = \pm 1/2$. These points correspond to the two eigenstates $|\pm\rangle$ so it is evident that the measurement term encourages collapse to one of the two eigenstates of the measurement operator.

Herein lies the clearest statement of the difference between our model and that considered in Ref. [13]. [The above equation for the dynamics of the Bloch vector compares directly to their Eq. (3.9).] Our model incorporates the collapse of the wave function in a natural way as a direct outcome of the interaction between a pseudoclassical meter and the system of interest. Also, the fact that our nonselective master equation preserves the probability distribution for $\hat{\sigma}_z$ ensures that the system tends towards each eigenvalue with the correct probability, unlike the model of Bonilla and Guinea [13].

In Fig. 6 we show typical trajectories of the system with various measurement strengths Γ. Specifically, we

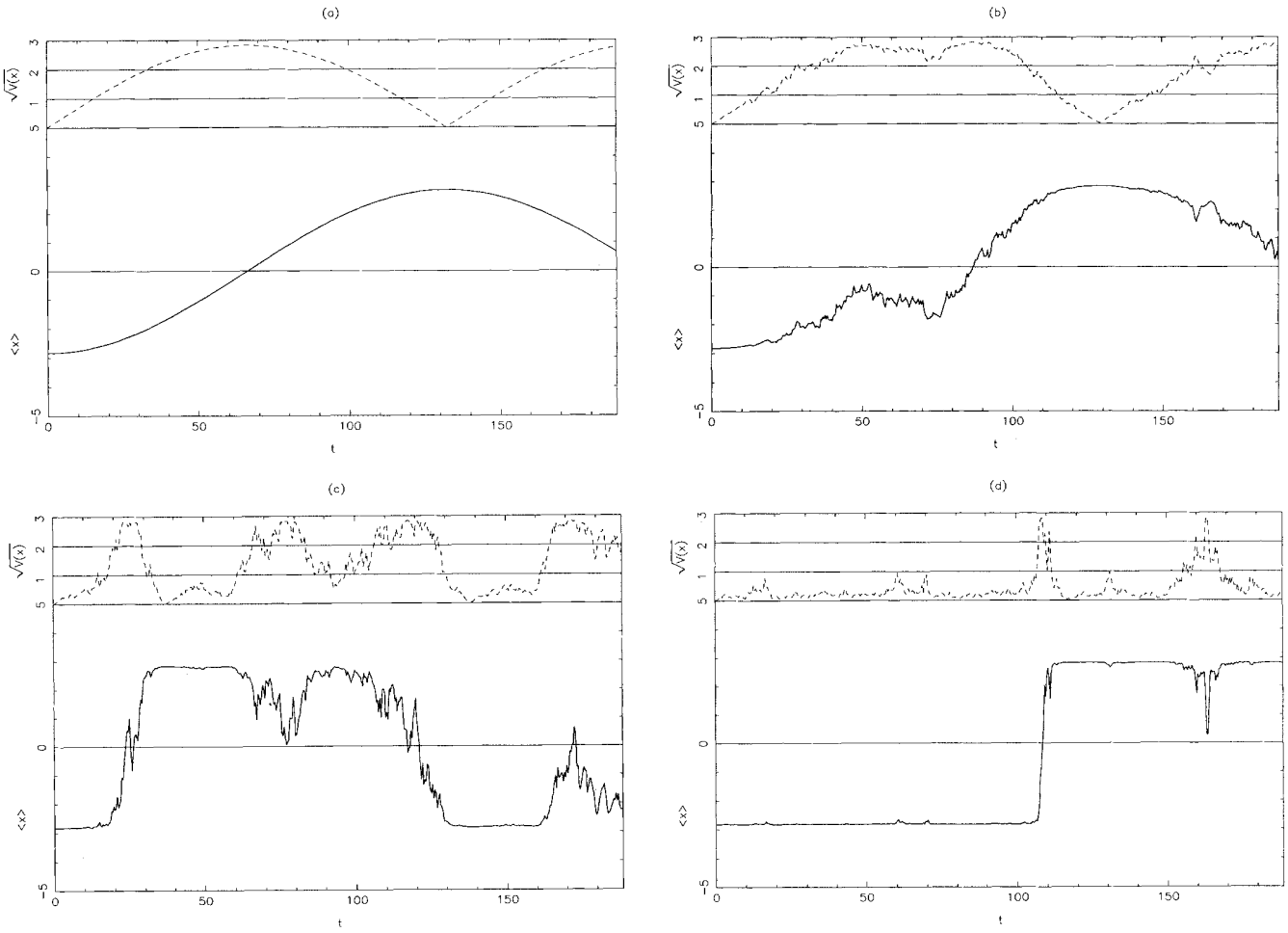

FIG. 6. The two-level approximation. Plot of typical selective evolution of the mean and standard deviation of the position of a continuously monitored particle under the two-level approximation. (a) For $\Gamma = 0$ the particle tunnels unitarily from one minima to the other. (b) For $\Gamma = 0.0003$, some "random walking" is seen but the particle's motion is still largely dominated by the unitary terms. As Γ increases [(c) $\Gamma = 0.003$ and (d) $\Gamma = 0.01$] the behavior of the particle changes to a "random-telegraph"-type evolution. The quantum Zeno effect is evident in the enhanced trapping of the particle in the left well for large Γ.

show the mean and variance of the position of the particle (which is given by the Z component of the Bloch vector). These trajectories show a strong similarity to those found from the full ponderomotive model. For $\Gamma = 0$ we see the unitary evolution of the particle as it tunnels from one minima to the other. For $\Gamma = 0.0003$ we still see tunneling due to the unitary evolution, but there is some noise superimposed, especially around the time when the particle is not localized in either well. As Γ increases we discern a gradual elimination of the unitary evolution. For large Γ the particle undergoes a "random-telegraph"-type evolution. The quantum Zeno effect is evident in the enhanced time of trapping of the particle in the left well for large Γ.

We now turn our attention to the deterministic terms in this stochastic equation. These terms are those resulting from the nonselective evolution in Eq. (3.13). The evolution of this two-level system in the nonselective case has been extensively studied [12]. With an initial state $|-\rangle$ $[X(0) = Y(0) = 0, Z(0) = -1/2]$, the general solution is

$$\begin{aligned} X(t) &= 0, \\ Y(t) &= -\frac{\Delta}{2\Omega} e^{-8D\Gamma t} S(\Omega t), \\ Z(t) &= -\frac{1}{2\Omega} e^{-8D\Gamma t} \left[8D\Gamma S(\Omega t) + \Omega C(\Omega t) \right], \end{aligned} \tag{3.16}$$

where we have $\Omega = \sqrt{|(8D\Gamma)^2 - \Delta^2|}$ and for $8D\Gamma < \Delta$ we set $S(\Omega t) = \sin \Omega t, C(\Omega t) = \cos \Omega t$ and for $8D\Gamma > \Delta$ we set $S(\Omega t) = \sinh \Omega t, C(\Omega t) = \cosh \Omega t$.

This nonselective evolution is shown in Fig. 7. We plot the nonselective evolution of the average value of $\langle \hat{x} \rangle$ for a particle initially well localized in the left well. We vary the measurement parameter Γ. Under free evolution, for $\Gamma = 0$ we see coherent tunneling from one well to the other. As the measurement parameter is increased this unitary evolution is gradually damped. Indeed, for $8D\Gamma > \Delta$ oscillations cease, and the particle probability density gradually diffuses from the left well. For very large Γ the survival time of the particle in the left-hand well is enhanced due to the nonselective measurement. This is the nonselective quantum Zeno effect. Of course this result applies to the real particle only as long as we are able to successfully model the system with a discrete measurement basis.

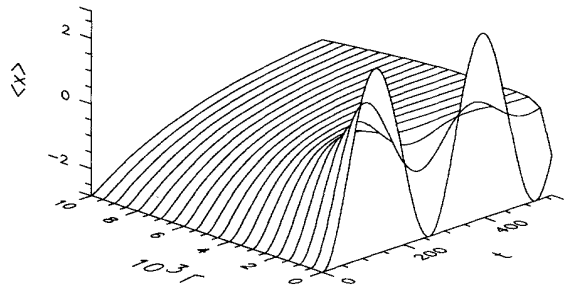

FIG. 7. Plot of the nonselective evolution of the average value of position $\langle \hat{x} \rangle$ for a particle for various values of the measurement parameter Γ. As the measurement parameter increases the free oscillations of unitary evolution become increasingly damped. For very large Γ the survival time of the particle in the left-hand well is significantly enhanced, which is how the quantum Zeno effect is manifest in the nonselective case.

In all nonselective measurement regimes $\Gamma > 0$ the particle will evolve to the long-time mixed state $\rho_{\rm NS}(\infty) = \frac{1}{2} I$. Such a state can be considered as made up of an ensemble of selectively measured systems. For weak measurements each individual system is undergoing tunneling with added noise due to the measurement backaction, as seen in Fig. 6(b). The effect of this noise is to cause different elements of the ensemble to become dephased. This is the origin of the damped oscillation seen in the nonselective (ensemble) evolution. In the strong measurement limit the measurement backaction dominates the evolution, causing the particle to act as a two-state "random telegraph." This can be shown by considering the nonselective evolution of the system as above. In this case, we expect that the evolution is well described by rate equations with equal transition probabilities between the wells. That is, we should get an equation of the form

$$\dot{\rho}_{11} = -\dot{\rho}_{22} = -R\rho_{11} + R\rho_{22}. \tag{3.17}$$

Now, in the limit of large Γ, Eq. (3.16) gives the following:

$$Z(t) \approx -\tfrac{1}{2} \exp\left(-\frac{\Delta^2}{16D\Gamma} t \right). \tag{3.18}$$

Since $Z = \frac{1}{2}(\rho_{22} - \rho_{11})$, we see that this equation is compatible to the rate equation [Eq. (3.17)] if we set the random-telegraph transition rate to be

$$R = \frac{\Delta^2}{32D\Gamma}. \tag{3.19}$$

This demonstrates the clearest possible manifestation of the quantum Zeno effect in that the transition probability is inversely proportional to the measurement parameter.

IV. CONCLUSION

We have constructed a general model for the measurement interaction between a quantum system and single pseudoclassical meter. The meter is pseudoclassical in the sense that its mass is so large that it always has a well-defined position and velocity. The system-meter interaction Hamiltonian is the usual von Neumann one. The meter state is measured innaccurately at regular intervals. By carefully choosing the parameters, it is possible to take the limit of continuous measurements. Our central equation is a stochastic Schrödinger equation which describes the selective evolution of the system state under measurement. This equation conditions the system state on the measurement result, and tends to cause the system to collapse towards an eigenstate of the measured quantity. Feedback on the meter constrains it to behave as an ideal laboratory pointer, tracking the position of

the system. It is the interpretation in terms of a realistic coupling to a single finite meter which we believe has not previously been published.

The model is applied to monitoring the position of a particle in a double-well potential. This system exhibits different behavior depending on the relative strength of the measurement. The free particle tunnels coherently from one well to the other. With weak measurement, the tunneling persists, but with diffusive noise added. This noise causes dephasing of the tunneling within the ensemble of pure state trajectories, which leads to damped oscillations in the ensemble average (represented by a density operator). As the measurement becomes stronger, coherent tunneling is replaced by incoherent flipping. This is a manifestation of the quantum Zeno effect, as the average time the particle remains stuck in its initial well increases approximately linearly with the measurement strength. This finding contradicts a recent claim by Fearn and Lamb [11] that there is no Zeno effect in a continuously monitored particle in a double-well potential. The nonselective evolution in this case exhibits overdamping. For very strong measurements, the energy of the particle increases so quickly that it does not remain localized in either well for any significant length of time, and so the Zeno effect cannot be observed. We believe that it is this last type of behavior which was produced by the measurement model of Lamb and Fearn, leading them to the wrong conclusion.

APPENDIX: NUMERICAL METHOD OF SIMULATION

In this appendix we describe the numerical method used for solution of the stochastic Schrödinger Eq. (2.18) in the double well. As long as the particle is not too energetic, we can use a truncated basis to model the system. Rather than use the eigenstates of the Hamiltonian, we choose to work in the well-known number-state basis for a harmonic-oscillator potential centered at the origin. Such states are complete and have the position representation of

$$\langle x|n\rangle = \pi^{-\frac{1}{4}}(2n!)^{-\frac{1}{2}}H_n(x)e^{-x^2/2}, \tag{A1}$$

where $H_n(x)$ is a Hermite polonomial. We transform to the operators

$$\begin{aligned}\hat{x} \to \hat{X} &= \frac{1}{\sqrt{2}}(a + a^\dagger),\\ \hat{p} \to \hat{Y} &= -\frac{i}{\sqrt{2}}(a - a^\dagger),\end{aligned} \tag{A2}$$

with the appropriate transformations of the free Hamiltonian. The initial state of the particle is $|-\rangle$, which is localized in the left minimum of the double-well potential. This state is readily calculated in the number state basis. For computational purposes we must eventually truncate our number-state basis. The validity of this truncation can be immediately assessed by noting that the initial state is well approximated by a coherent state $|\alpha\rangle$ located at $\alpha \approx -2\sqrt{D}$. As usual, this state has a number-state expansion peaked about the mean $\bar{n} \approx 4D = 4$. This suggests that a truncation of the number basis at about 40 would be adequate. In this case the problem is quite manageable on a computer.

* Electronic mail address:gagen@physics.uq.oz.au
† Electronic mail address:wiseman@physics.uq.oz.au
‡ Electronic mail address:milburn@physics.uq.oz.au

[1] W. Pauli, *General Principles of Quantum Mechanics* (Springer-Verlag, Berlin, 1980).
[2] B. Misra and E.C.G. Sudarshan, J. Math. Phys. **18**, 756 (1977).
[3] A. Peres, Am. J. Phys. **48**, 931 (1980).
[4] E. Joos, Phys. Rev. D **29**, 1626 (1984).
[5] C.M. Caves and G.J.Milburn, Phys. Rev. A **36**, 5548 (1987).
[6] N. Gisin, Phys. Rev. Lett. **52**, 1657 (1984); **53**, 1776 (1984); Helv. Phys. Acta. **62**, 363 (1989).
[7] L. Diosi, Phys. Lett. A **120**, 377 (1987); **129**, 419 (1988); **132**, 233 (1989).
[8] L. Diosi, Phys. Rev. A **40**, 1165 (1989).
[9] P. Pearle, Phys. Rev. A **39**, 2277 (1989).
[10] V.P. Belavkin and P. Staszewski, Phys. Rev. A **45**, 1347 (1992).
[11] H. Fearn and W.E. Lamb, Jr., Phys. Rev. A **46**, 1199 (1992).
[12] G.J. Milburn, J. Opt. Soc. Am. B **5**, 1317 (1988).
[13] L.L. Bonilla and F. Guinea, Phys. Rev. A **45**, 7718 (1992).
[14] J. von Neumann, *Mathematische Grundlagen der Quanten-mechanik* (Springer, Berlin, 1932), especially Chap. 6 [English translation: *Mathematical Foundations of Quantum Mechanics* (Princeton University Press, Princeton, NJ, 1955)].
[15] W. Heisenberg, *The Physical Principles of Quantum Mechanics* (The University of Chicago Press, Chicago, 1930).
[16] H.M. Wiseman and G.J. Milburn, Phys. Rev. A **47**, 1652 (1993).
[17] N. Gisin and I.C. Percival, Phys. Lett. A **167**, 315 (1992); J. Phys. A **25**, 5677 (1992).
[18] C.W. Gardiner, A.S. Parkins, and P. Zoller, Phys. Rev. A **46**, 4363 (1992).
[19] A.O. Caldeira and A.J. Leggett, Ann. Phys. (N.Y.) **149**, 374 (1983), **153**, 445(E) (1983).
[20] A.J. Leggett, S. Chakravarti, A.T. Dorsey, M.P.A. Fisher, A. Garg, and W. Zwerger, Rev. Mod. Phys. **59**, 1 (1987).
[21] F. Grossmann, P. Jung, T. Dittrich, and P. Hänggi, Z. Phys. B **84**, 315 (1991).